structure types can be viewed as deriving from the successive dismantling of the three-dimensional adamantine structure of HgS[19] as it attempts to accommodate the varying amounts of added A_2Q. For example the μ_4-coordination of the Q^{2-} ions in the HgQ structure is reduced to μ_3- and μ_2-coordination in $[Hg_6Q_7]_n^{2n-}$ and to only μ_2-coordination in $[Hg_3Q_4]_n^{2n-}$. Another phase that also belongs to this homologous family is K_6HgQ_4[20] ($n = 3$, $m = 1$), which features discrete tetrahedral $[HgQ_4]^{6-}$ units (the HgQ lattice has been reduced to individual $[HgQ_4]^{6-}$ units). This is very similar to the successive breakup of the structures of the main-group elements (e.g., Si, P) that ensues upon reduction with very electropositive metals to form the familiar Zintl phases.[21]

The results reported here show that the three-dimensional structure of HgQ is tractable and can accommodate various amounts of alkali-metal monosulfides. It is likely that the A_2Q/HgQ system constitutes an infinitely adaptive pair similar to the $(ZnS)_n(In_2S_3)_m$[22] and $(BaS)_n(FeS)_m$[23] systems. Work to identify other members of this family is continuing. In conclusion, using alkali-metal polychalcogenides as solvents and reagents is a viable synthetic and crystal growth route to novel chalcogenide solid-state materials.

Acknowledgment. Financial support from the Center for Fundamental Materials Research (CFMR) Michigan State University and the National Science Foundation for a Presidential Young Investigator Award, CHE-8958451, is gratefully acknowledged.

Supplementary Material Available: Tables of atomic coordinates of all atoms and anisotropic and isotropic thermal parameters of all non-hydrogen atoms, bond distances and angles, and a figure with the atomic labeling of $K_2Hg_6S_7$ (7 pages); a listing of calculated and observed ($10F_o/10F_c$) structure factors (14 pages). Ordering information is given on any current masthead page.

(19) Toshikazu, O. *J. Appl. Crystallogr.* **1974**, *7*, 396-397.
(20) Sommer, H.; Hoppe, R. Z. *Anorg. Allg. Chem.* **1978**, *443*, 201-211.
(21) (a) von Schnering, H.-G.; Nönle, W. *Chem. Rev.* **1988**, *88*, 243-273. (b) von Schnering, H.-G. *Angew. Chem., Int. Ed. Engl.* **1981**, *20*, 33-51. (c) Schafer, H. *Ann. Rev. Mater. Sci.* **1985**, *15*, 1-41.
(22) (a) Donika, F. G.; Kiosse, G. A.; Radautsan, S. I.; Semiletov, S. A.; Zhitar, V. F. *Sov. Phys. Crystallogr.* **1968**, *12*, 745-749. (b) Boorman, R. S.; Sutherland, J. K. *J. Mater. Sci.* **1969**, *4*(8), 658-671. (c) Barnett, D. E.; Boorman, R. S.; Sutherland, J. K. *Phys. Status Solidi A* **1971**, *4*(1), K49-K52.
(23) (a) Grey, I. E. *J. Solid State Chem.* **1974**, *11*, 128-134. (b) Cohen, S.; Rendon-DiazMiron, L. E.; Steinfink, H. *J. Solid State Chem.* **1978**, *25*, 179-187. (c) Hoggins, J. T.; Steinfink, H. *Acta Crystallogr., Sect. B* **1977**, *33*, 673-678.

Articles

Reactivity of Metal Oxides Cu_2O, MnO, CoO, NiO, CuO, and ZnO with Indialite

G. Pourroy,* J. L. Guille, and P. Poix

I.P.C.M.S. Groupe de Chimie des Matériaux Inorganiques UM 380046 E.H.I.C.S., 1 rue Blaise Pascal BP 296, 67008 Strasbourg Cedex, France

Received May 24, 1989

Reactivities of Cu_2O, MnO, CoO, NiO, CuO, and ZnO with indialite ($Mg_2Al_4Si_5O_{18}$) are studied under air, argon, or vacuum and for temperatures between 800 and 1150 °C, by using X-ray diffraction, magnetic measurements, and ESR spectroscopy. While Cu_2O is inert toward indialite, MO oxides always react: small quantities of cupric oxide disappear in indialite phase at about 950–1000 °C under air and appear again partly above 1030 °C. Magnetic measurements and ESR spectroscopy prove that the oxidation degree of dissolved copper is 2+ and that this dissolved copper does not behave as copper in cupric oxide. For greater concentrations of CuO, a spinel phase appears. The other MO oxides always destroy the indialite framework, giving M_2SiO_4 and a spinel phase for manganese, cobalt, and nickel oxides, α-SiO_2, $MgSiO_3$, and $ZnAl_2O_4$ in the zinc case.

Introduction

Until now, cordierite ($Mg_2Al_4Si_5O_{18}$) has given rise to a rich literature because of its unusual physical properties. Its relatively low polycrystalline linear thermal expansion α_p (1×10^{-6}–4×10^{-6}/°C), low dielectric constant (4–6), and high volume resistivity (>10^4 Ω cm) make it attractive for catalyst carriers and application in electronic packaging.

Mg cordierite exists under three polymorphic forms: a hexagonal high-temperature form, named indialite or α-cordierite, isostructural with beryl (space group $P6/mmc$), an orthorhombic low-temperature form designed β-cordierite (space group $Cccm$) which is the most encountered structure for natural cordierite, and a metastable form, μ-cordierite.[1-3] The hexagonal and orthorhombic structures are characterized by their six-membered rings of tetrahedrally coordinated cations (T_2) perpendicular to the c axis. Alternate layers of the hexagonal ring structure are connected through Mg octahedra and T_1 tetrahedra (Figure 1). Silicon occupies mostly T_2 tetrahedra, and aluminum T_1 tetrahedra. Differences between high- and

(1) Karkhanavala, M. D.; Hummell, F. A. *J. Am. Ceram. Soc.* **1953**, *36*(12), 389-92.
(2) Gibbs, G. V. *Am. Mineral.* **1966**, *51*, 1068-87.
(3) Meagher, E. P.; Gibbs, G. V. *Can. Mineral.* **1977**, *15*, 43-49.

0897-4756/90/2802-0101$02.50/0

Table I. Experimental Conditions for Different Mixtures of Metal Oxide-Indialite: Metal Concentration, Heating and Cooling Atmospheres, Temperatures and Times of Annealing, Color and Grinding Characteristics of the Obtained Pellets, and Phases Detected in the X-ray Spectra Recorded at Room Temperature

oxides	mol ratio r [metal oxide]/ [indialite]	heating atm	cooling atm	annealing temp, °C	annealing time, h	color	grinding	phases detected by XRD
MnO	1	vacuum	vacuum	950	1	light green	easy	indialite, Mn_2SiO_4, spinel
CoO	1	vaccum	vacuum	1100	5	pink	easy	
Co_3O_4	1	air	vacuum	1050	5	pink	easy	indialite, Co_2SiO_4, spinel
	1	air	air	1050	5	pink	easy	
NiO	1	air	air	1050	4	light green	easy	indialite, Ni_2SiO_4, spinel
CuO	0.25	air	air	900	1	dark red	difficult	indialite, CuO
	0.25	air	air	1000	1	white	difficult	indialite
	0.25	air	air	1040	3	dark red	difficult	indialite, CuO
	0.25	air	argon	1040	3	orange	difficult	indialite, Cu_2O
	2	air	air	1040	17	dark red	difficult	indialite, CuO, Cu_2O, spinel
Cu_2O	1	vacuum	vacuum	1040	5	orange	easy	indialite, Cu_2O, Cu
ZnO	1	air	air	1000	2	white	easy	indialite, $ZnAl_2O_4$, Zn_2SiO_4
	1	air	air	1150	1	white	easy	indialite, α-SiO_2, $ZnAl_2O_4$, $MgSiO_3$

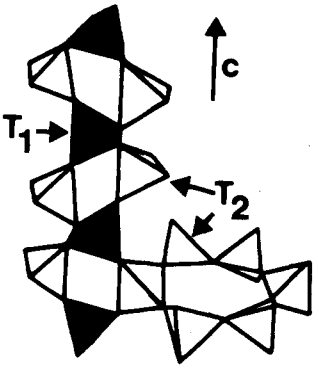

Figure 1. Arrangement of tetrahedra and octahedra in the cordierite structure. Each T_2 tetrahedron in the rings is joined via a T_1 tetrahedron (full) to the ring above and the ring below such that all tetrahedra are corner sharing. Octahedra link two rings in the same plane (after Putnis et al.[5]).

low-temperature cordierites lie in a greater or lesser degree of disorder between the aluminum and silicon atoms within T_1 and T_2 sites.[3-5] As for the metastable form, it exhibits a stuffed high-quartz structure.[6,7]

Most natural cordierites are not pure Mg cordierite but contain other cations such as Fe^{2+}, Fe^{3+}, Li^+, Mn^{2+}, Be^{3+}, or molecules Na_2O or H_2O, which either substitute for Mg^{2+}, Al^{3+}, and Si^{4+} or are inserted in the channel sites of cordierite framework.[8-11] For instance, Mössbauer studies performed on natural iron cordierite show that of the 1.85 wt % iron content, 79 wt % is present as Fe^{2+} replacing Mg^{2+} in the octahedral sites, 20 wt % as Fe^{2+} within the large channel sites, and 1 wt % as Fe^{3+} replacing Al^{3+} in the T_1 sites.[12,13]

Many attempts at synthesizing chemical derivatives and investigating their structures were performed. The introduction of cations at oxidation degree +1, Cs^+ or K^+, in the large structural cavity of the channels of the cordierite framework produces a change in the Al^{3+}/Si^{4+} ratio.[14] Modifications of the thermal expansion behavior were observed in high-temperature cordierite in which Mn^{2+}, Ga^{3+}, or Ge^{4+} partly substitute for Mg^{2+}, Al^{3+}, and Si^{4+}.[11] The unique complete metal substitution occurs with cobalt in the solid solutions $Mg_xCo_{1-x}Al_4Si_5O_{18}$ ($0 \leq x \leq 1$).[15]

All these studies concern syntheses of new cordierite compounds but never focus on the reactivity of metals with cordierite. The latter is of a great importance in the electronic packaging industry. Recent studies have been performed on titanium cordierite interfaces using X-ray photoelectron spectroscopy (XPS) to probe the reactivity at the Ti–cordierite interface for varying Ti coverage, postdeposition annealing, and substrate temperature during deposition.[16] Ti reacts strongly with the cordierite surface, reducing the Si–O bonds at low coverages and the Al–O bonds at higher coverages. Copper–cordierite interfaces have also given rise to several works. Starting cordierite is either a glass or a sol–gel precursor.[17-20] The latter, used in our previous works, gives μ-cordierite between 850 and 900 °C and the indialite phase between 950 and 1050 °C. It is found in that case, that a satisfactory copper–cordierite cosintering, with a sufficient strong metal-to-ceramic bonding, occurs only in an oxidizing atmosphere. The final temperature must be above the copper–oxygen eutectic temperature (1065 °C) and must be raised quickly between 200 and 1070 °C (800 °C h^{-1}). Copper diffusion through ceramic substrate and chemical modifications at the interface compared to the bulk composition are observed.[18] Only the indialite phase is present near the surface, whereas indialite and μ-cordierite as well as $MgAl_2O_4$ traces are present in the bulk. So, to bring enlightenment on mechanisms and phases involved in the elaboration of copper–cordierite interfaces, we drastically reduce the system: we report here about the reactions between powders of copper oxides and indialite. This study is then extended to other transition-metal oxides MO (M = Mn, Co, Ni, and Zn).

(4) Putnis, A. *Contrib. Mineral. Petrol.* **1980**, *74*, 135–141.
(5) Putnis, A.; Colin, A. F.; Gobbi, G. C. *Phys. Chem. Minerals* **1985**, *12*, 211–6.
(6) Schreyer, W.; Schairer, J. F. *Z. Kristallogr.* **1961**, *116*, 60–82.
(7) Langer, K.; Schreyer, W. *Am. Mineral.* **1969**, *54*, 1442–59.
(8) Goldman, D. S.; Rossman, G. R. *Am. Mineral.* **1977**, *62*, 1144–57.
(9) Parkin, K. M.; Loeffler, B. M.; Burns, R. G. *Phys. Chem. Minerals* **1977**, *1*, 301–11.
(10) Armbruster, T. *Z. Kristallogr.* **1986**, *174*, 205–17.
(11) Ikawa, H.; Otagiri, T.; Imai, O.; Suzuki, M.; Urabe, K.; Udagawa, S. *J. Am. Ceram. Soc.* **1986**, *69*, 492–8.
(12) Duncan, J. F.; Johnston, J. H. *Aust. J. Chem.* **1974**, *27*, 249–57.
(13) Johnston, J. H.; Duncan, J. F. *Chem Geol.* **1976**, *17*, 27–35.
(14) Evans, D. L.; Fischer, G. R.; Geiger, J. E.; Martin, F. W. *J. Am. Ceram. Soc.* 1980, *63*, 629–34.
(15) Wandschneider, P.; Seifert, F. *J. Am. Ceram. Soc. C* **1984**, 163.
(16) Bortz, M.; Ohuchi, F. S. *J. Appl. Phys.* **1988**, *64*(4), 2054–58.
(17) Poetzinger, J. E.; Risbud, S. M. *J. Phys.* **1985**, *46*, C4 147–151.
(18) Oliver-Broudic, V.; Guille, J.; Bernier, J. C.; Han, B. S.; Werckmann, J.; Faerber, J.; Humbert, P.; Carriere, B. *Mater. Sci. Eng. A* **1989**, *A109*, 77–81.
(19) Allen, G. D.; Risbud, S. H. *J. Electron. Mat.* **1987**, *16*(6), 423–426.
(20) Risbud, S. H.; Allen, G. D.; Poetzinger, J. E. *Mater. Sci. Res.* **1987**, *21*, 359.
(21) Tanabe, K. *Catal. Sci. Technol.* **1981**, *2*, 231.
(22) O'Keeffe, M.; Stone, F. S. *J. Phys. Chem. Solids* **1962**, 23, 261–266.

Experimental Section

A sol–gel precursor of indialite is submitted to six annealings of 24 h at 1300 °C separated by grindings until no change in the indialite X-ray spectra is observed. Metal oxides ZnO, NiO, and copper oxides are powders of purity greater than 99.9%. MnO is obtained by reduction of Mn_2O_3 under H_2 at 1000 °C. Decomposition of cobalt carbonate $CoCO_3$ at 600 °C gives cobaltic cobaltous oxide Co_3O_4. Cobaltous oxide CoO is obtained by heating Co_3O_4 at 1000 °C and cooling the powder under dried argon.

Powders of metal oxide and indialite are ground together carefully and compacted. Samples are submitted to several thermal treatments, under different heating and cooling atmospheres, air, argon, or vacuum. For attempts under air or argon, the pellets are put on an indialite bed in a pythagoras crucible, so that the contacts between the pellets and the support are as small as possible. Pellets containing MnO, Cu_2O, and CoO are introduced in a silica tube sealed under vacuum. Numerous attempts have been performed, the molar ratios r = [metal oxide]/[indialite] changing from 0.1 to 10, the reaction temperatures from 800 to 1150 °C, and the annealing times from 1 to 17 h. Only the attempts $r = 1$ are presented in Table I for manganese, cobalt, nickel, and zinc monooxides and Cu_2O, similar results being obtained for other values of r. For cupric oxide, phases detected by X-ray diffraction are not identical for r lower or higher than 0.25. All the treatments are followed by quenching to room temperature except for samples cooled under argon atmosphere. Annealing times widely exceed reaction time required for interfaces elaboration to emphasize reactions occurring at the interface.

The samples are investigated by X-ray diffraction, magnetic measurements, and electron spin resonance. X-ray diffraction patterns are taken at room temperature using a Kristalloflex Siemens diffractometer and cobalt radiation. Cell parameters and intensity diffraction lines are measured by using NaCl as internal standard. For the latter measurements, the same weights of annealed doped indialite and dried NaCl are carefully mixed and spread over the sample holder in order to keep a constant ratio between NaCl and doped indialite. Magnetic susceptibility measurements are performed with a pendulum type magnetometer in the temperature range 4.2–300 K. The susceptibility is calculated for 1 mol of the mixture $Mg_2Al_4Si_5O_{18}$–metal oxide. Electron spin resonance measurements are recorded at room temperature on weakly doped samples (1 mol % CuO) using a Brucker ER 200 D X-band spectrometer.

Results

The pellets present different aspects, according to the oxide involved, its concentration, and the thermal treatment. Changes of color are sometimes observed. For instance, cobalt samples become mauve. For low concentrations of CuO ($r \leq 0.25$), the pellets, dark at room temperature, become white at 950–1000 °C and dark red again above 1030 °C. When the samples heated to 1040 °C are cooled under an argon atmosphere, they get the orange color of Cu_2O. Grindings are not difficult except for CuO samples heated above 900 °C.

X-ray diffraction measurements performed on the grounded pellets show that the studied oxides always react with indialite at temperatures between 900 and 1150 °C except Cu_2O. Depending on the thermal treatment, different reactions occur: either the indialite structure is destroyed and new phases appear (for manganese, cobalt, nickel, and zinc oxide), or metal oxide disappears in the indialite framework (for cupric oxide). Nothing noticeable is observed on the samples Cu_2O–indialite heated under vacuum, only a partial decomposition of Cu_2O in Cu metal (Table I).

Reactivity of MnO, CoO, NiO, and ZnO with Indialite ($r = 1$). As soon as metal oxides MO (M = Mn, Co, Ni, and Zn) react with indialite, new compounds appear:

For M = Mn, Co, and Ni, M_2SiO_4 is detected while the whole metal oxide has not disappeared yet. In cobalt case, the result is the same, whatever the starting oxide may be, since Co_3O_4 transforms into CoO above 800 °C. However, CoO coming from Co_3O_4 reacts more rapidly, likely because CoO grains are smaller. At the end of reaction, neither MgO nor Al_2O_3 appear in X-ray diffraction patterns, but the spinel phase $MgAl_2O_4$ does. For a molar ratio r, the reaction is written

$$rMO + Mg_2Al_4Si_5O_{18} \rightarrow (r/2)M_2SiO_4 + (r/5)MgAl_2O_4 + (1 - r/10)Mg_2Al_4Si_5O_{18} \quad \text{(I)}$$

However, nothing allows us to assert that spinel phase is pure $MgAl_2O_4$. Indeed, its diffraction lines are too large to conclude from accurate measurements of cell parameters.

For zinc oxide, the results are completely different since its reaction with indialite gives α-SiO_2, $MgSiO_3$, and $ZnAl_2O_4$ from following the reaction:

$$rZnO + Mg_2Al_4Si_5O_{18} \rightarrow (3r/2)\alpha\text{-}SiO_2 + rMgSiO_3 + rZnAl_2O_4 + (1 - r/2)Mg_2Al_4Si_5O_{18} \quad \text{(II)}$$

Intermediate phases are observed at 1000 °C. Their diffraction lines seem to correspond to Zn_2SiO_4.

Reactivity of CuO. What happens between CuO and indialite is more unusual, compared with the reactions described previously. Cupric oxide diffraction lines appear in X-ray spectra of weak doped CuO–indialite samples, $r \leq 0.25$, after annealings at 900 °C, but become weaker after annealing at 950 °C and disappear after annealing at 1000 °C (Table I). CuO is detected again when the samples are heated to 1040 °C but is characterized by large diffraction lines. At the same time, the intensities of indialite diffraction lines have been measured, as well as the intensities of NaCl added following the method done in the Experimental Section. No fundamental changes of the intensities are observed in the indialite spectra except a slight decrease (15%) of the 102 reflection line. Furthermore, no significant variation of cell parameters is observed. Another fact is noteworthy: for $r < 0.25$, Cu_2O diffraction lines appear in the spectra of samples heated to 1040 °C when cooled under argon. SEM examinations show Cu_2O parallelepipeds of less than 1-μm caught in the indialite grains (Figure 2). Last, a complete reduction of all copper oxide dissolved in the indialite phase into metallic copper is obtained at 600 °C under hydrogen atmosphere.

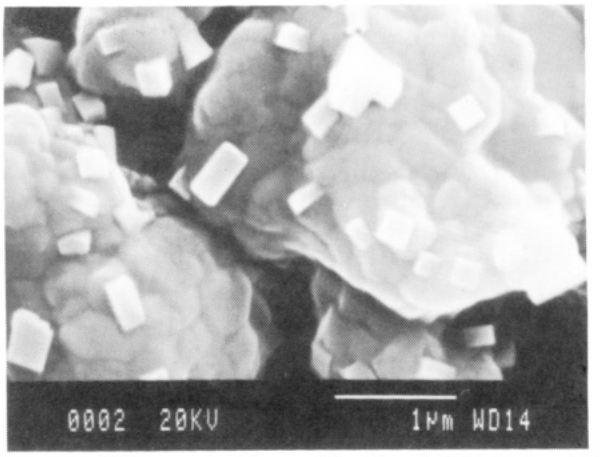

Figure 2. SEM examinations of the 25 mol % CuO-doped indialite heated at 1040 °C and cooled under argon.

The limit value of r, for which cupric oxide totally disappears (i.e., no more CuO diffraction lines) after an annealing up to 1000 °C is 0.25. The molar susceptibility of the sample containing 25 mol % of CuO and heated to 1000 °C follows a Curie–Weiss law, $\chi = 0.14/(T + 11)$, above 100 K (Figure 3). At lower temperatures, the

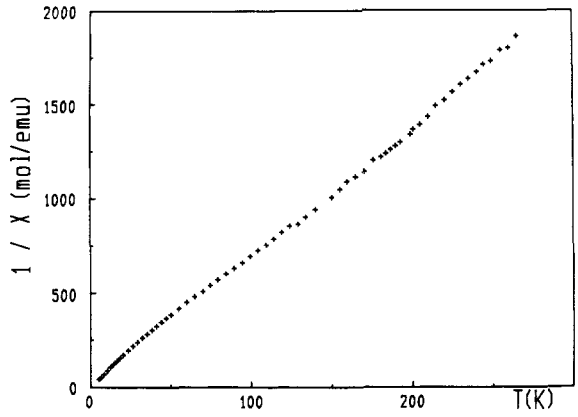

Figure 3. Inverse susceptibility of the 25 mol % CuO-doped indialite heated at 1000 °C and cooled under air.

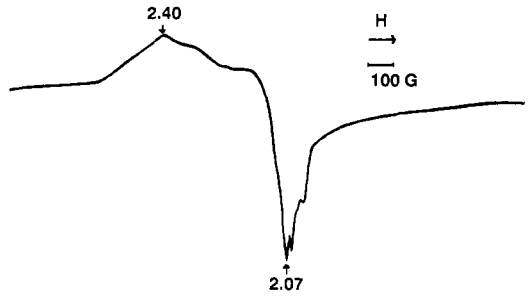

Figure 4. ESR spectrum at room temperature of 1 mol % CuO-doped indialite annealed at 1000 °C.

magnetic moment χT decreases when the temperature decreases. The ESR signal of no heated sample containing 1 mol % CuO is very weak since CuO is antiferromagnetic. It increases for samples annealed at 1000 °C and presents shape and g values similar to those obtained for copper dispersed on alumina[23] (Figure 4). No change in the signal shape is observed by heating the sample up to 1040 °C, indicating that, at very low concentrations, the copper state does not seem to change between 1000 and 1040 °C. Nevertheless, a decrease of solubility is observed on samples containing 20 and 25 mol % CuO. An accurate estimation of the amount of cupric oxide thrown out of the indialite phase above 1040 °C is difficult, since it begins to evolve at this temperature.

For molar ratios above 1 and for temperatures higher than 1040 °C, the indialite structure partly destroys. CuO, Cu_2O, and a spinel phase, probably the solid solution $Cu_xMg_{1-x}Al_2O_4$, are detected in the X-ray spectra. SiO_2 does not appear; it is probably not crystallized yet.

Discussion

Indialite ($Mg_2Al_4Si_5O_{18}$) reacts with the metal oxides MnO, NiO, CoO, CuO, and ZnO and not with Cu_2O. Little amounts of metal oxide MO ($r \simeq 0.2$ in eq I and II) are sufficient to lead to the formation of new compounds except for CuO. For $r = 2$, great amounts of CuO have not reacted yet at 1040 °C after an annealing of 17 h, while 1–5 hours are needed to obtain a complete disappearing of other MO metal oxides. These observations allow us to conclude that MnO, NiO, CoO, and ZnO are more agressive toward indialite than CuO.

According to the resulting compounds, the reactions can be divided into two groups, those leading to a compound of olivine structure M_2SiO_4 and a spinel phase formulated $Mg_{1-x}M_xAl_2O_4$ (M = Mn, Ni, and Co), and those leading to $MgSiO_3$ and MAl_2O_4 (M = Zn). These two different behaviors are related to the competition between the metals for octahedral and tetrahedral sites. Silicon has a strong affinity for tetrahedral sites, so that M_2SiO_4 and $MgSiO_3$ compounds are better obtained. Zn^{2+} also prefers a tetrahedral environment as it is encountered in ZnO, ZnS, and the zinc spinel compounds such as $ZnFe_2O_4$. Its affinity for tetrahedral sites is greater than that of magnesium, so $MgSiO_3$ and $ZnAl_2O_4$ are preferentially formed in the zinc case. An opposite behavior is encountered for Mn^{2+}, Co^{2+}, and Ni^{2+}, which leave magnesium in a tetrahedral environment. So, compounds of olivine structure in which the metal M has an octahedral environment and the magnesium aluminate spinel are better obtained. However, nothing allows us to assert that the latter phase is not a solid solution $Mg_{1-x}M_xAl_2O_4$ (M = Mn, Co, Ni, Cu). Its diffraction lines are very large, so that an accurate calculation of cell parameters is impossible. Cupric oxide has a behavior close to that of Mn^{2+}, Ni^{2+}, and Co^{2+}, with respect to the compounds obtained at high temperature, although no silicon compounds crystallize.

The chemical reactions between metal oxides and indialite can be considered from another point of view, the competition between entities more-or-less acidic or basic. The oxides involved can be listed according to their increasing acidity MgO, Al_2O_3, SiO_2, and MgO, ZnO.[21] So, in the zinc case, a reaction between the most basic and the most acidic is observed, giving thus $MgSiO_3$. A classification between MgO on one hand and MnO, CoO, and NiO on the other is more difficult. Nevertheless, a thermodynamic study of the equilibrium

$$MO + MgCl_2 \underset{2}{\overset{1}{\rightleftharpoons}} MCl_2 + MgO \quad (M = Mn, Co, Ni)$$

shows that the reaction 1 is favored. The behavior of MnO, CoO, and NiO is quite the same with respect to MgO in our case, since M_2SiO_4 (M = Mn, Co, Ni) compounds are better obtained. However, such a classification changes according to the reaction temperature. That is probably why intermediate phases, not very well-defined, are encountered in the zinc case.

Cupric oxide has a particular behavior toward indialite. At low concentration, r = [CuO]/[indialite] ≤ 0.25, its X-ray diffraction lines disappear when the mixture is heated to 1000 °C. Two reasons may be produced to explain that:

A dissolution of cupric oxide in the indialite framework, either substituted for metals or inserted in channel sites as often encountered in natural Mg cordierite. That might be responsible for the decrease of 102 reflection line intensity. However, a metal substitution would lead to the formation of MgO, Al_2O_3, or SiO_2, which is not observed. Nevertheless, MgO is hardly detectable by X-ray diffraction measurements, since its most intensive diffraction lines are superimposed to the 114 and 312 reflections of indialite.

A dissolution of cupric oxide in an amorphous phase. Nevertheless, some facts are inconsistent with that assertion: starting indialite samples have been heated to 1300 °C for 6 days to allow all the compound to be crystallized, and copper favors the crystallization as observed in copper cordierite cosintering. Furthermore, indialite diffraction lines intensities do not decrease except one of them.

Anyway, it can be asserted that copper is bounded to the indialite matrix in these samples, since it reduces into metallic copper at 600 °C under hydrogen atmosphere (200 °C for a copper oxide powder). Magnetic studies show that dissolved copper is under Cu^{2+} form: the sample $r = 0.25$

(23) Lumbeck, H.; Voitlaender, J. *J. Catal.* **1969**, *13*, 117.

presents a paramagnetic behavior characterized by a Curie constant, $C = 0.55$ for 1 mol of Cu^{2+}, close to the theoretical one ($C_{th} = 0.375$). The large maximum observed above 200 K in the susceptibility curve of CuO disappears, showing that the distance between copper ions is greater in our sample than in CuO. ESR spectra confirm this oxidation degree for copper and show that the copper environment changes by heating the mixture. The shape of the signal indicates that copper is in an axial site. More accurate ESR studies are needed to conclude about the environment, the temperature for which the reaction begins and the quantities of CuO dissolved in the indialite framework.

The solubility of cupric oxide decreases above 1030 °C. Indeed, CuO diffraction lines, missing in the X-ray diffraction pattern of sample $r = 0.25$ heated to 1000 °C, appear again on heating it above 1030 °C. But they are much larger, indicating that the grains, arising from the oxidation of small-sized Cu_2O parallelepipeds on cooling, are much smaller than those of the CuO starting powder. This decrease of copper solubility is probably linked to the reduction of Cu^{2+} to Cu^{+}.

Acknowledgment. We thank J. C. Broudic, I.P.C.M.S. G.M.I. UM 380046, E.H.I.C.S. Strasbourg for supplying indialite sol-gel precursor and helpful discussions, and E. Coronado, Departamento Quimica Inorganica, Facultad Ciencias Quimicas, Burjasot, Spain, for recording ESR spectra.

Registry No. Cu_2O, 1317-39-1; MnO, 1309-48-4; CoO, 1307-96-6; NiO, 1313-99-1; CuO, 1317-38-0; ZnO, 1314-13-2; $Mg_2Al_4Si_5O_{18}$, 12026-18-5; $MgAl_2O_4$, 12068-51-8; Mn_2SiO_4, 13568-32-6; Co_2SiO_4, 13455-33-9; Ni_2SiO_4, 13775-54-7; $ZnAl_2O_4$, 12068-53-0; Zn_2SiO_4, 13597-65-4; SiO_2, 7631-86-9; $MgSiO_3$, 13776-74-4; indialite, 61027-88-1.

Rare-Earth Ions Adsorbed onto Porous Glass: Luminescence as a Characterizing Tool

M. F. Hazenkamp* and G. Blasse

Physics Laboratory, University of Utrecht, P.O. Box 80000, 3508 TA Utrecht, The Netherlands

Received July 24, 1989

The luminescence properties of some rare-earth (Ln) ions adsorbed on porous vycor glass (PVG) are reported. The results are used to characterize this system. Vibronic sidebands of the Gd^{3+} $^6P_{7/2} \rightarrow {}^8S_{7/2}$ emission due to coupling with vibrations of the water molecule and of silica are observed. This observation indicates that the Ln ions are bound to the surface of the pores of PVG and that they are coordinated on the other side by water molecules. From the decay time of Eu^{3+} on PVG, the number of coordinating water molecules is determined by using Horrocks' formula. This number is approximately 4. The energy transfer from Ce^{3+} to Tb^{3+} and from Gd^{3+} to Tb^{3+} is studied. From the dependence of the transfer efficiency on the acceptor concentration, an estimation of the mean distance between two adsorbed in Ln ions is made. This distance is about 7 Å. Ce^{3+} and Eu^{3+} are observed to quench each other's luminescence. The maximum quenching distance is determined to be about 14 Å.

Introduction

Research on the luminescence properties of ions and molecules at solid surfaces is a relatively new subject. Interesting work in this field was done by Anpo et al.,[1] who studied the photoluminescence of heterogeneous catalysts activated with transition-metal complexes. Other work was done on the luminescence of rare-earth ions (with or without an organic complex) adsorbed onto porous vycor glass by Mack and Reisfeld[2,3] and by Blasse et al.[4]

In this paper we present a closer examination of the luminescence properties of some rare-earth ions adsorbed on porous vycor glass. Moreover, we show some cases of interaction between adsorbed rare-earth ions. We will use the results to characterize this system. It was found that luminescence is a suitable tool to provide a qualitative and, to a certain extent, quantitative picture of the structure of the investigated system.

Experimental Section

Sample Preparation. Samples were prepared by impregnating pieces of porous vycor glass (PVG) with aqueous solutions of rare-earth (Ln) ions. The starting materials used were Eu_2O_3, Gd_2O_3, La_2O_3, Tb_4O_7, and $Ce_2(CO_3)_3 \cdot 5H_2O$ (Highways Int. 99.99%). PVG (Corning 7930) is a porous material consisting of 96% SiO_2 and 4% B_2O_3. The internal surface consists of silanol groups. The average pore size is 40 Å, and the BET surface area is about 150 m^2/g.[5] All solutions were prepared by dissolving the Ln salts in hydrochloric acid (Merck P.A.). The concentration of the Ln ions in the solutions was always 0.8 M. By use of this high concentration, the adsorption equilibrium is shifted to the side of the porous glass and the concentration of Ln ions in the pores of PVG is expected to be maximal. When a larger mean distance between the luminescent ions was desired, a part of these ions was replaced by La^{3+} ions. The pH of the impregnating solutions was approximately 0.

Disk-shaped pieces of PVG, 1 mm thick and 10 mm in diameter, were cleaned by boiling for several hours in aqueous 30% H_2O_2

(1) Kubokawa, Y.; Anpo, M. *Adsorption and Catalysis on Oxide Surfaces*; Che, M., Bond, G. C., Eds.; Elsevier Science Publishers: Amsterdam, 1985; p 127.
(2) Mack, H.; Reisfeld, R.; Avnir, D. *Chem. Phys. Lett.* **1983**, *99*, 238.
(3) Reisfeld, R.; Manor, N.; Avnir, D. *Sol. Energy Mater.* **1983**, *8*, 399.
(4) Blasse, G.; Dirksen, G. J.; van der Voort, D.; Sabbatini, N.; Perathoner, S.; Lehn, J.-M.; Alpha, B. *Chem. Phys. Lett.* **1988**, *146*, 347.
(5) Corning technical information.

0897-4756/90/2802-0105$02.50/0